

## Design of a Miniaturized Dual-Band Bandpass Filter with High Selectivity

Xiao Lei Ma<sup>\*</sup>, Yong Lun Luo, Shuang Lin Yuan, and Long Chen

**Abstract**—In this paper, a miniaturized dual-band bandpass filter with high selectivity and band-to-band isolation is presented. The filter consists of two quarter-wavelength stepped impedance resonators (SIRs) which share a common grounded via-hole and two symmetrical half-wavelength SIRs which are embedded into the inner space to reduce the size of the filter. Two independent mixed coupling paths which are created by the coupling between these SIRs introduce two different passbands. Five transmission zeros (TZs) are generated near the two passbands to achieve high frequency selectivity and band-to-band isolation. To validate the design theory, a dual-band filter operating at 2.45 and 5.2 GHz was designed and fabricated. The size of the proposed filter only occupies  $0.095\lambda_g \times 0.109\lambda_g$  and the measured 3 dB fractional bandwidth (FBW) of the first and second passbands is 11.5% and 7.4% respectively. The measured results are in good agreement with the simulated results.

### 1. INTRODUCTION

In the process of rapid development in microwave wireless communication, the requirements for multi-band/multi-functional microwave systems that support various modern services have increased rapidly. To meet the requirements, various dual-band bandpass filters (BPFs), as the key components in dual-band wireless communication systems, have been studied and developed. In order to obtain a dual-band passband, many methods have been explored. In [1], two single-band filters are paralleled to achieve two passbands. In [2], two passbands are achieved through cascading a broadband filter with a bandstop structure. In [3, 4], the synthesis approach including frequency transformations and coupling matrix optimizations is used to design dual-band BPF. In [5–8], a dual-band BPFs using SIRs and stub loaded resonators with multiple resonant modes have been proposed. However, these conventional methods show many disadvantages: complicated structure, large size and hard to design, which can not satisfy the requirements of the modern communication systems. Hence, many researchers have concentrated on the design of dual-band bandpass filters which have good frequency selectivity, compact and high isolation [9–15].

In this paper, a miniaturized dual-band BPF which consists of two quarter-wavelength stepped impedance resonators and two symmetrical half-wavelength stepped impedance resonators is proposed. Through the coupling between these SIRs, two independent mixed coupling paths which can introduce two different passbands are created. Meanwhile, because of the mixed electric/magnetic (EM) coupling, multiple TZs are generated near the passbands. Owing to these TZs, the BPF achieves good passband selectivity and satisfactory band-to-band isolation. The center frequencies and the bandwidths of the two passbands can be controlled independently.

---

*Received 15 April 2014, Accepted 5 June 2014, Scheduled 7 June 2014*

<sup>\*</sup> Corresponding author: Xiao Lei Ma (xiaoleima1988@163.com).

The authors are with the Research Institute of Electronic Science and Technology, University of Electronic Science and Technology of China, Chengdu 611731, China.

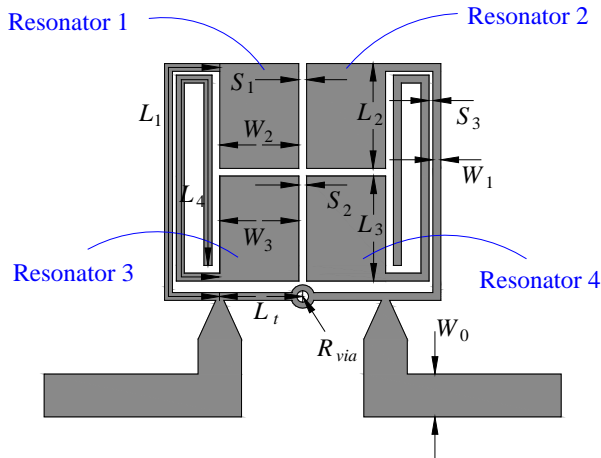
## 2. DESIGN AND ANALYSIS OF PROPOSED BPF

Figure 1 shows the layout of the proposed dual-band BPF. The filter consists of four stepped impedance resonators: two quarter-wavelength SIRs and two symmetrical half-wavelength SIRs. The two quarter-wavelength SIRs share a common grounded via-hole and another two symmetrical half-wavelength SIRs are embedded into the inner space, as shown in Figure 1. The grounded via-hole offers the magnetic coupling and the gap  $S_1$  between the low-impedance lines of resonators 1 and 2 provide the electric coupling. The electric coupling between the low-impedance lines of resonators 3 and 4 is achieved through the gap  $S_2$ . It must be emphasized that the magnetic coupling between resonators 3 and 4 is introduced through the coupling between the resonators 3, 4 and a part of high-impedance transmission line of resonators 1, 2, and also with the effect of the grounded via-hole. The corresponding coupling and routing scheme of the proposed filter is equivalent to a structure chart as shown in Figure 2. A graded feed line allows flexibility in the design, and the feed location can be easily adjusted.

As shown in Figure 2, two passbands are realised by introducing two mixed coupling paths between the input and output port. The first passband is introduced by the mixed coupling path which is created between resonators 1 and 2. The second passband is introduced by the mixed coupling path which is created between the resonators 3 and 4. The widths of the two passbands are mainly influenced by the strength of the electric coupling between the SIRs and the strength of the electric coupling can be controlled through turning the gap  $S_1$  and  $S_2$ . In order to verify the proposed method, a dual-band BPF design whose two passbands are centered at 2.45 and 5.2 GHz separately applied in wireless local area network is proposed. In this BPF design, the main procedure is that two passbands of the filter are designed separately in the first step. Then, the two designs are combined together. Simulated by Ansoft's High Frequency Structural Simulator (HFSS) v10, the whole structure was optimized and tuned in the last step.

Firstly, a traditional mixed-coupled structure [16] is designed for the first passband, and the center frequency of which is 2.45 GHz, as shown in Figure 3. In this design, the center frequency of the passband can be controlled by changing the size of two SIRs, and the bandwidth can also be changed by controlling the strength of the electric coupling in the structure. Figure 4 shows the simulated results of the BPF in Figure 3. As shown in Figure 4, two TZs are introduced near the passband. TZ<sub>1</sub> at the low frequency end of the passband is realised by mixed electric and magnetic coupling effects, and TZ<sub>2</sub> in the high frequency end is introduced by the harmonic effects of the distributed transmission line in the filter.

Then, the second mixed-coupled structure is designed to achieve the second passband, for which the center frequency is 5.2 GHz. Figure 5 shows the layout of the second design. The two embedded SIRs achieve the electric coupling through the gap  $S_2$  while the magnetic coupling is achieved through the



**Figure 1.** Layout of the proposed dual-band filter.

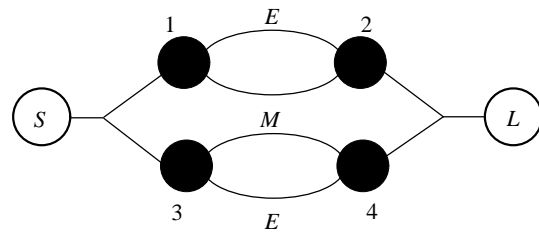


**Figure 2.** Corresponding coupling and routing scheme of the proposed filter.

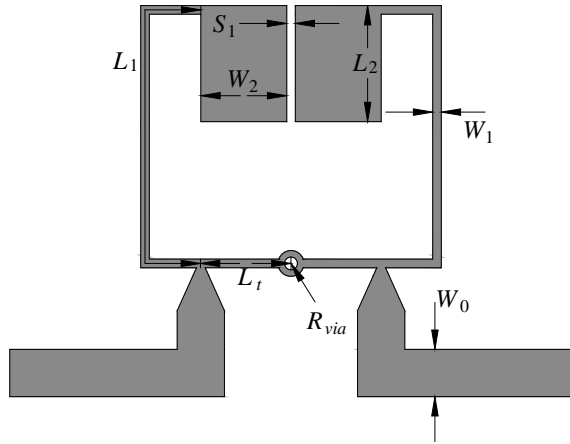


Figure 3. Layout of the 2.45 GHz BPF.

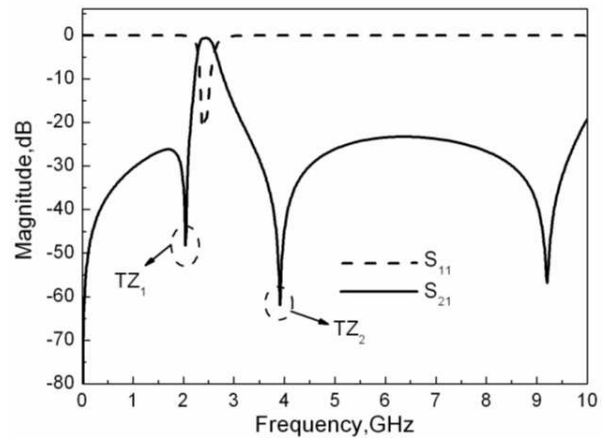


Figure 4. Simulation results of the 2.45 GHz BPF.

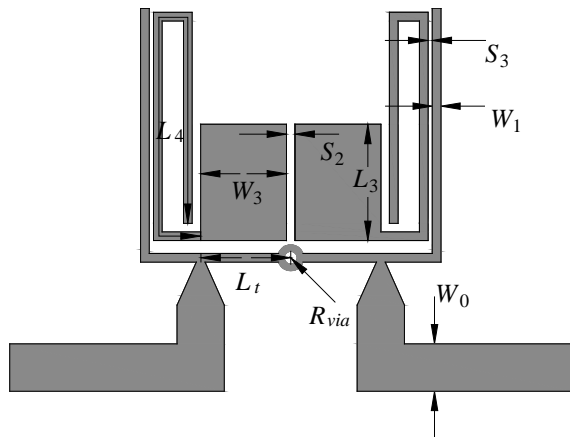


Figure 5. Layout of the 5.2 GHz BPF.

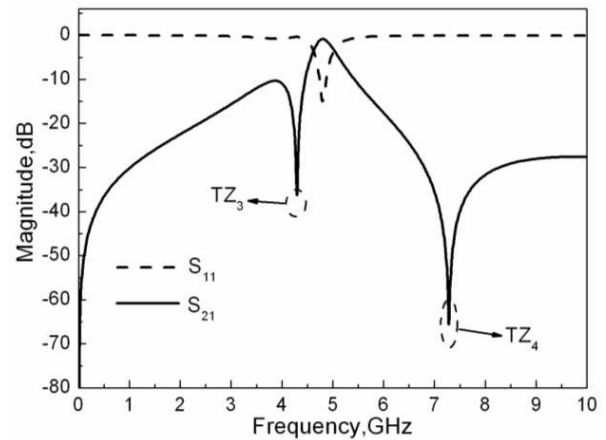
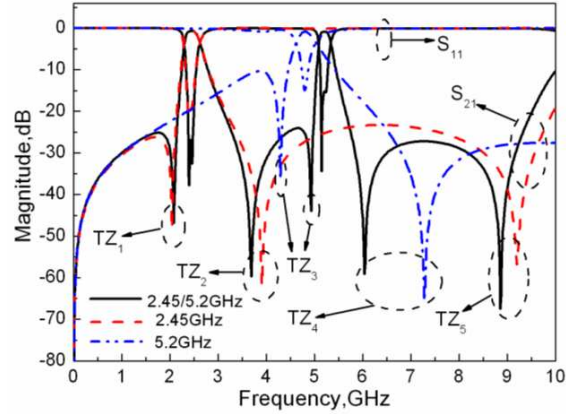


Figure 6. Simulation results of the 5.2 GHz BPF.

grounded via-hole in the coupled line. The simulated result of the second design is shown in Figure 6. As shown in Figure 6, two TZs are introduced near the passband. The TZ<sub>3</sub> located at the low frequency end is realised by the mixed electric and magnetic coupling, and TZ<sub>4</sub> at the high frequency end is introduced by the harmonic effects of the distributed transmission line in the filter.

A new structure then can be achieved by combining the two filters designed above, as shown in Figure 1. Simulated by the optimization function of HFSS v10, the main parameters, such as  $S_1$ ,  $S_2$ ,  $S_3$  and  $L_t$ , achieve the optimal values. After optimization, a good simulated result of the dual-band structure is achieved. Compared with the two single-band structures, the simulated  $S$ -parameters of the dual-band structure are shown in Figure 7. It can be seen that five transmission zeros are introduced near the two passbands. TZ<sub>1</sub> is generated by the canceling effects of the mixed coupling in the first coupling path, and TZ<sub>2</sub> is generated by the harmonic effects of the transmission line of the resonators 1 and 2. TZ<sub>3</sub> near the second passband is generated by the canceling effects of the mixed coupling in the second coupling path. Figure 8 depicts the simulated electric field distribution at the center frequencies of the two passbands. As shown in Figure 8, the electric field distributes in the outer and inner SIRs, respectively, and the electric field distribution at 2.45 GHz mainly concentrates on the outer SIRs while the electric field distribution at 5.2 GHz mainly concentrates on the inner SIRs. It can be verified that the first passband is created by the outside SIRs, and the second passband is introduced by the inside SIRs.



**Figure 7.** Comparison of the simulation results of the dual-band filter and the two single-band filters.

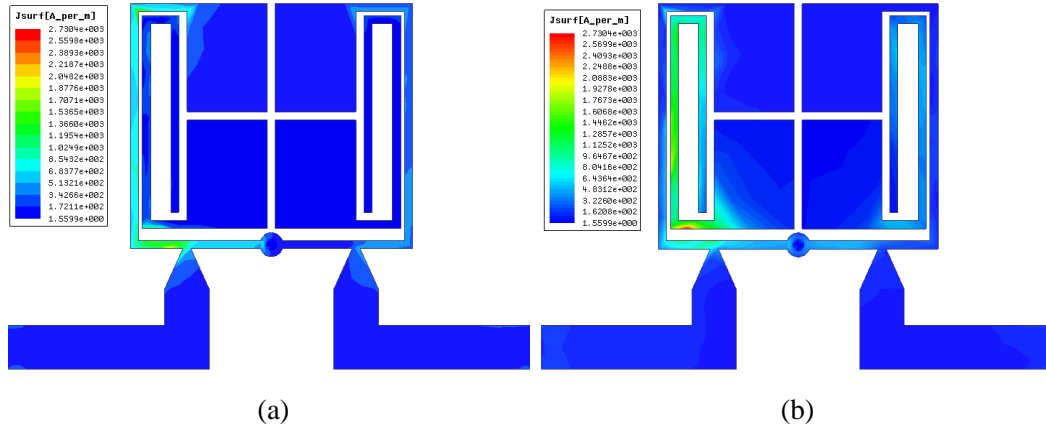


**Figure 8.** Electric field distribution of the dual-band filter: (a) 2.45 GHz and (b) 5.2 GHz.

### 3. FILTER FABRICATION AND MEASURED RESULTS

Figure 9 shows the photograph of the fabricated dual-band filter. The proposed filter is fabricated on the Rogers RO4350 substrate with a relative dielectric constant of 3.66 and a thickness of 0.508 mm. The dimensions of proposed filter were:  $W_0 = 1.10$  mm,  $W_1 = 0.20$  mm,  $W_2 = 2.00$  mm,  $W_3 = 2.00$  mm,  $L_1 = 8.60$  mm,  $L_2 = 2.70$  mm,  $L_3 = 2.70$  mm,  $L_4 = 12.40$  mm,  $L_t = 2.40$  mm,  $S_1 = 0.19$  mm,  $S_2 = 0.22$  mm,  $S_3 = 0.10$  mm,  $R_{via} = 0.20$  mm. The total area of proposed BPF is  $6.10 \times 7.00$  mm<sup>2</sup> which corresponds to  $0.095\lambda_g \times 0.109\lambda_g$ , where  $\lambda_g$  is the guided wavelength at the centre frequency of the first passband. The filter was tested using an Agilent E8363B network analyzer. Comparison of simulated and measured results of the dual-band filter is shown in Figure 10. The measured results show that the first passband is centered at 2.43 GHz, and the second passband is centered at 5.2 GHz. The return loss is better than 14.2 dB in the first passband and better than 12.2 dB in the second passband. The measured 3 dB fractional bandwidths for the first and second passbands are 11.5% and 7.4%, respectively. The measured insertion losses for the first and second passbands are 2.3 dB and 2.5 dB, respectively. The transmission zeros, TZ<sub>1</sub>, TZ<sub>2</sub>, TZ<sub>3</sub>, TZ<sub>4</sub>, TZ<sub>5</sub>, are located at 1.95 GHz with 43.8 dB rejection, 3.62 GHz with 49.2 dB rejection, 5.21 GHz with 31.5 dB rejection, 5.8 GHz with 46.3 dB rejection, 9.76 GHz with 49.2 dB rejection, respectively. The frequency selectivity and band-to-band isolation of the dual-band filter are obviously improved by TZs introduced near the two passbands. The measured results agree well with the simulated ones. However, the measured bandwidth of the second passband is narrower than the simulated one, and the insertion loss of the filter becomes bigger than the simulation result, as shown in Figure 7. This may be caused by fabricated errors in the microstrip

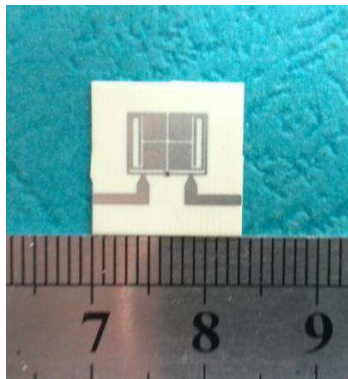


**Figure 9.** Photograph of the fabricated dual-band bandpass filter.

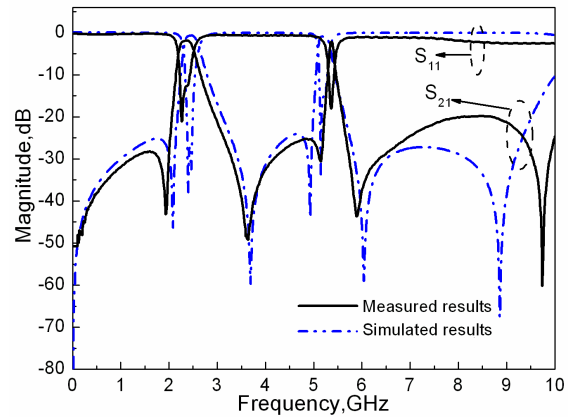


**Figure 10.** Comparison of simulated and measured results of the dual-band filter.

**Table 1.** Comparisons with other proposed BPFs.

Ref.	Center Frequency $f_0$ (GHz)	Insertion loss (dB)	3dB FBW (%)	Transmission zero location (GHz)	Circuit size ( $\lambda_g \times \lambda_g$ )
[13]	2.4/5.16	0.6/1.4	13.7/6.3	1.95, 2.7, 4.6, 5.4	$0.46 \times 0.42$
[14]	1.575/2.4	0.9/1.1	6/3.8	1.1, 2.0, 3.2	$0.5 \times 0.35$
[15]	0.9/2.45	1.1/1.0	6/4.8	0.78, 1.05, 1.82, 2.26, 3.2	$0.2 \times 0.13$
This work	2.45/5.2	2.3/2.5	11.5/7.4	1.95, 3.62, 5.21, 5.8, 9.76	$0.095 \times 0.109$

line and the dimension of the gaps in these SIRs. Table 1 summarizes the comparison of the proposed filter with other reported bandpass filters [13–15].

#### 4. CONCLUSION

In this paper, a miniaturized dual-band BPF operated at 2.45 and 5.2 GHz with high selectivity and isolation is presented. Two independent mixed coupling paths are introduced by the coupling between the SIRs which are designed in this filter. Because of the two independent mixed coupling paths, the center frequencies and bandwidths of the two passbands can be independently controlled. Owing to the mixed coupling, multiple TZs are introduced near the passbands to enhance the band-to-band isolation and frequency selectivity. The theory proposed has been verified by simulation and measurement. With good frequency performance and small size (i.e.,  $6.10 \times 7$  mm), the filter is attractive in WLAN dual-band (i.e., 2.45 and 5.2 GHz) applications.

#### REFERENCES

- Chen, C. Y. and C. Y. Hsu, “A simple and effective method for microstrip dual-band filters design,” *IEEE Microw. Wireless Compon. Lett.*, Vol. 16, No. 5, 246–248, May 2006.
- Tsai, L. C. and C. W. Hsue, “Dual-band bandpass filters using equal-length coupled-serial-shunted lines and Z-transform technique,” *IEEE Trans. Microw. Theory Tech.*, Vol. 52, No. 4, 1111–1117, Apr. 2004.
- Guan, X., Z. Ma, P. Cai, Y. Kobayashi, T. Anada, and G. Hagiwara, “Synthesis of dual-band bandpass filters using successive frequency transformations and circuit conversions,” *IEEE Microw. Wireless Compon. Lett.*, Vol. 16, No. 3, 110–112, Mar. 2006.

4. Mokhtaari, M., J. Bornemann, K. Rambabu, and S. Amari, "Coupling matrix design of dual and triple passband filters," *IEEE Trans. Microw. Theory Tech.*, Vol. 54, No. 11, 3940–3946, Nov. 2006.
5. Chu, Q. X. and F. C. Chen, "A compact dual-band bandpass filter using meandering stepped impedance resonators," *IEEE Microw. Wireless Compon. Lett.*, Vol. 18, No. 5, 320–322, May 2008.
6. Zhang, X. Y., J. X. Chen, Q. Xue, and S. M. Li, "Dual-band bandpass filters using stub-loaded resonators," *IEEE Microw. Wireless Compon. Lett.*, Vol. 17, No. 8, 583–585, Aug. 2007.
7. Kuo, J. T., T. H. Yeh, and C. C. Yeh, "Design of microstrip bandpass filters with a dual-passband response," *IEEE Trans. Microw. Theory Tech.*, Vol. 53, No. 4, 1331–1337, Apr. 2005.
8. Mondal, P. and M. K. Mandal, "Design of dual-band bandpass filters using stub-loaded open-loop resonators," *IEEE Trans. Microw. Theory Tech.*, Vol. 56, No. 1, 150–155, Jan. 2008.
9. Sun, X. and E. L. Tan, "A novel dual-band bandpass filter using generalized trisection stepped impedance resonator with improved out-of-band performance," *Progress In Electromagnetics Research Letters*, Vol. 21, 31–40, 2011.
10. Li, Z. P., T. Su, Y. L. Zhang, and C. H. Liang, "A novel dual-band passband filter with controllable center frequencies and bandwidths," *Progress In Electromagnetics Research Letters*, Vol. 40, 29–38, 2013.
11. Zhang, X. Y., C. H. Chan, Q. Xue, and B.-J. Hu, "Dual-band bandpass filter with controllable bandwidths using two coupling paths," *IEEE Microw. Wireless Compon. Lett.*, Vol. 20, No. 11, 616–618, Nov. 2010.
12. Sun, S. J., L. Lin, B. Wu, K. Deng, and C. H. Liang, "A novel quad-mode resonator and its application to dual-band bandpass filter," *Progress In Electromagnetics Research Letters*, Vol. 43, 95–104, 2013.
13. Li, Y. C., H. Wong, and Q. Xue, "Dual-mode dual-band filter based on a stub-loaded patch resonator," *IEEE Microw. Wireless Compon. Lett.*, Vol. 21, No. 10, 525–527, Oct. 2011.
14. Chang, Y. C., C. H. Kao, M. H. Weng, and R. Y. Yang, "Design of the compact dual-band bandpass filter with high isolation for GPS/WLAN applications," *IEEE Microw. Wireless Compon. Lett.*, Vol. 19, No. 12, 780–782, Dec. 2009.
15. Zhang, X. Y., J. X. Chen, J. Shi, and Q. Xue, "High-selectivity dual-band bandpass filter using asymmetric stepped-impedance resonators," *Electron. Lett.*, Vol. 45, No. 1, 63–64, 2009.
16. Wei, X. B., Y. Shi, P. Wang, and J. X. Liao, "Design of compact, wide stopband bandpass filter using stepped impedance resonator," *Journal of Electromagnetic Waves and Applications*, Vol. 26, Nos. 8–9, 1095–1104, 2012.